Electronic Supplementary Information

Ir(III)- and Ru(III)-doped layered double hydroxides as affordable heterogeneous catalysts for electrochemical water oxidation

Lucia Fagiolari,[a,b] Francesco Zaccaria,[a] Ferdinando Costantino,[a] Riccardo Vivani,[c] Christos Mavrokefalos,[d] Greta R. Patzke[d,]* and Alceo Macchioni[a,]*

a) Department of Chemistry, Biology and Biotechnology, Università di Perugia and CIRCC- Via Elce di Sotto 8, I-06123 Perugia, Italy; b) Department of Applied Science and Technology, Politecnico di Torino - Corso Duca degli Abruzzi 24, I-10129 Torino, Italy; c) Department of Pharmaceutical Sciences, Università di Perugia - Via del Liceo 1, I-06123 Perugia, Italy; d) Department of Chemistry, University of Zurich, Winterthurerstrasse 190, CH-8057 Zurich, Switzerland. E-mail: alceo.macchioni@unipg.it, greta.patzke@chem.uzh.ch

- **Synthesis of M-LDHs**

The four M-LDHs used in this study were synthesized by mixing suitable amounts of the salts of the desired metals and urea in water, according to previously established methods.[1–3] Decarbonate water was obtained by refluxing distilled water under nitrogen flux prior to use; carrying out the synthetic reactions at the water reflux temperature further helps avoiding CO_2 contamination. In particular, the following procedures were used:

- *Synthesis of* ***B****.* 1.7494 g of $ZnCl_2$, 1.3287 g of $AlCl_3 \cdot 6H_2O$ and 1.3176 g of urea were dissolved in 37 ml of decarbonate CO_2-free water in a 50 ml round bottom flask. The solution was kept under stirring at refluxing temperature for 24 hours.
- *Synthesis of* ***Ir-1****.* 0.4171 g of $ZnCl_2$, 0.2714 g of $AlCl_3 \cdot 6H_2O$, 0.0755 g of $IrCl_3 \cdot 3.7H_2O$ and 0.3147 g of urea were dissolved in 9 ml of decarbonate CO_2-free water in a 25 ml round bottom flask. The solution was kept under stirring at refluxing temperature for 24 hours.
- *Synthesis of* ***Ru****.* 1.6900 g of $ZnCl_2$, 1.0689 g of $AlCl_3 \cdot 6H_2O$, 0.2146 g of $RuCl_3$ and 1.2755 g of urea were dissolved in 35 ml of decarbonate CO_2-free water in a 100 ml round bottom flask. The solution was kept under stirring at refluxing temperature for 24 hours.
- *Synthesis of* ***Ir-2****.* 0.2897 g of $MgCl_2$, 0.2624 g of $AlCl_3 \cdot 6H_2O$, 0.0794 g of $IrCl_3 \cdot 3.7H_2O$ and 0.3130 g of urea were dissolved in 9 ml of decarbonate CO_2-free water in a 25 ml round bottom flask. The solution was kept under stirring at refluxing temperature for 24 hours.

In all cases, a white powder precipitated after a few hours. The precipitate was filtered on a Gooch 4 vacuum filter and washed several times with decarbonate water, to eliminate unreacted salts. The so-obtained powders were dried at 60°C overnight.

- **Characterization of LDHs**

Powder X-ray diffraction (PXRD) patterns were collected on a STOE StadiP diffractometer, with a Cu tube operating at 40 kV and 40 mA, with a step size of 0.015° 2ϑ and a scan rate of 1 step/min, using Cu $K_{\alpha 1}$ radiation. Cell parameters of undoped and doped LDHs were determined by using the Rietveld method[4] implemented in the GSAS program.[5] First the background was refined with a 12 terms polynomial function, then profile parameters, including Gaussian and Lorentzian terms and asymmetry parameters were also refined. Atomic parameters were refined by constraining the chloride ions and water molecules at the same fractional coordinates. At the end of the refinement, the shifts in all parameters were less than their standard deviations. Rietveld plots are shown in Fig. S1-4.

The morphology of the samples was investigated using a Field Emission Scanning Electron Microscope Zeiss Supra 50VP, equipped with secondary, backscattered electron detector. To perform SEM, a small amount of powder was dispersed in pure methanol, sonicated for a few minutes, deposited in a SEM holder and dried overnight. ICP-OES analysis was performed with a Varian 700-ES series inductively coupled plasma-optical emission spectrometer in order to evaluate metal content. All the sample were dissolved with a few drops of fuming ultra pure HNO_3 and then diluted with Milli Q water. Supernatant solutions were filtered on a 0.2 µm filter, neutralized with fuming extra pure HNO_3 to pH 7 and then analysed. FT-IR spectra of the pure samples, stored at room temperature, were recorded on a Bruker VERTEX 70 FT-IR Spectrometer, with a resolution of 1 cm^{-1}, 16 scans and an acquisition range from 4000 to 400 cm^{-1}.

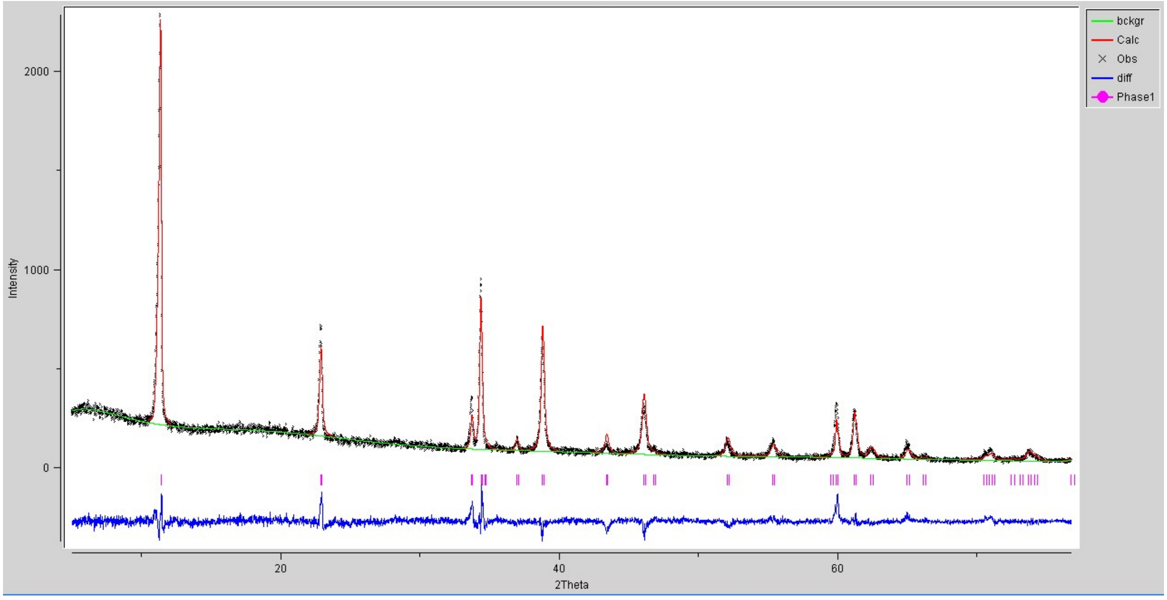

Fig. S1. Rietveld plot for B. Observed, calculated and difference profiles are shown. Peak positions are marked as purple lines**.**

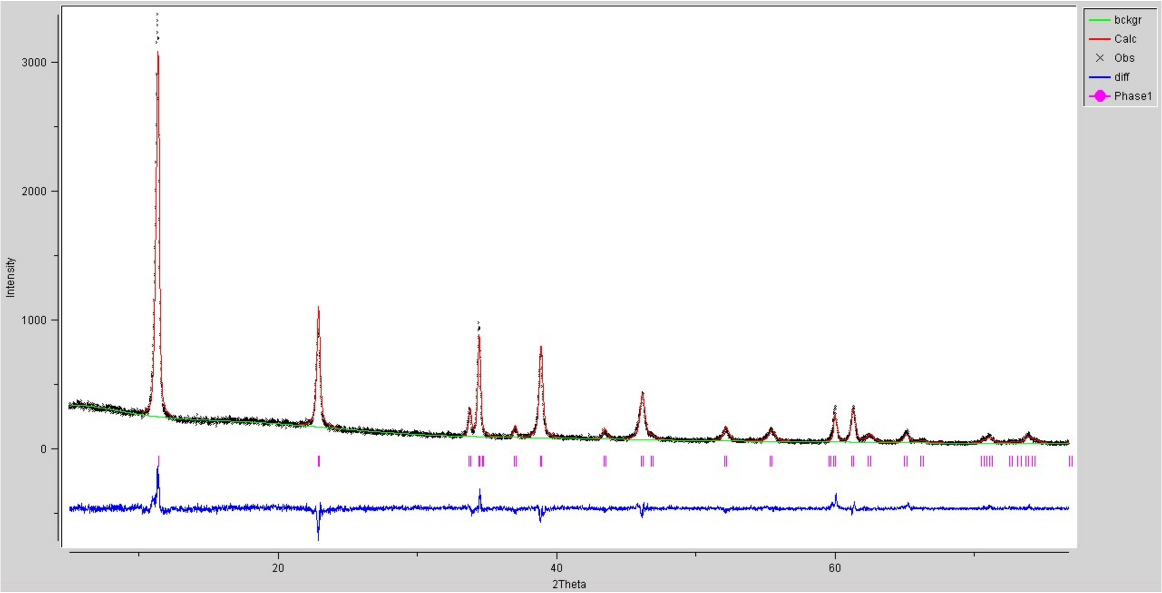

Fig. S2. Rietveld plot for **Ir-1**. Observed, calculated and difference profiles are shown. Peak positions are marked as purple lines.

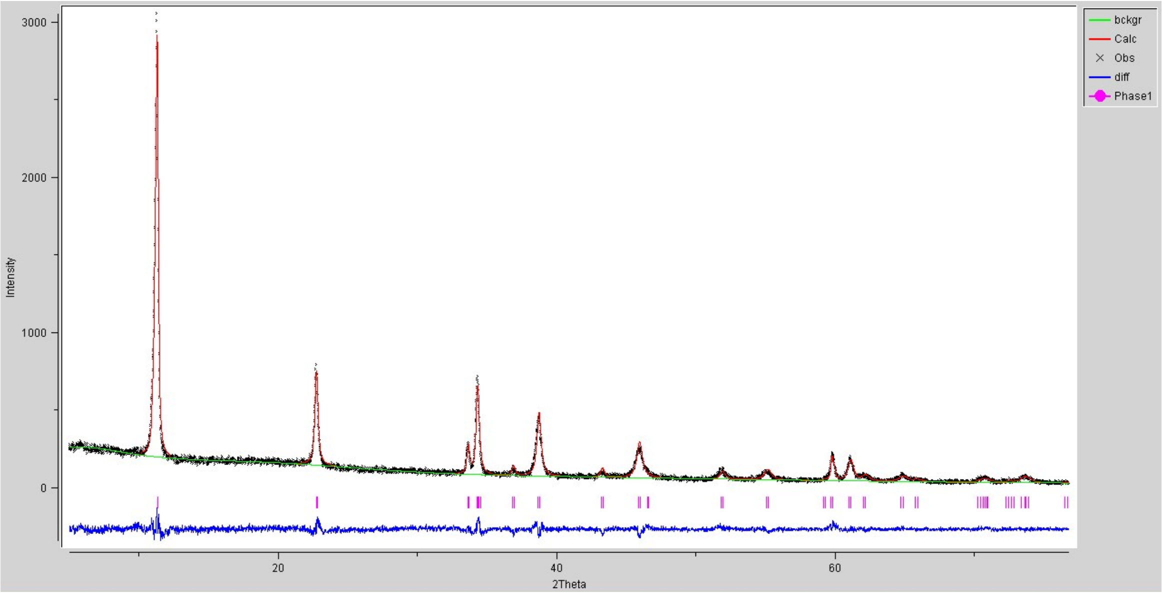

Fig. S3. Rietveld plot for **Ru**. Observed, calculated and difference profiles are shown. Peak positions are marked as purple lines.

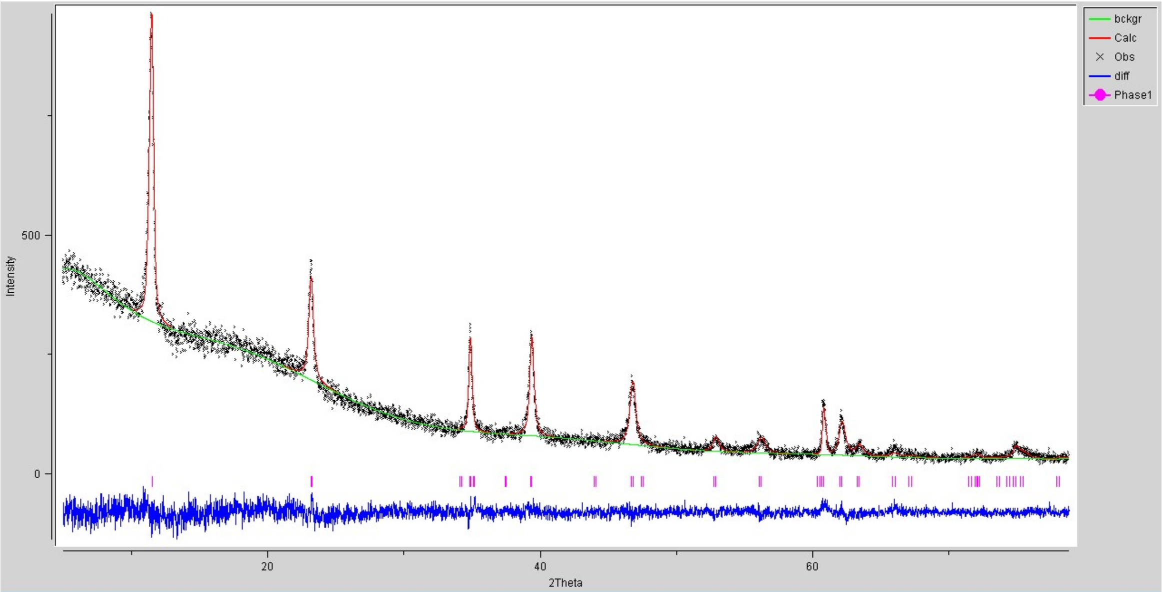

Fig. S4. Rietveld plot for **Ir-2**. Observed, calculated and difference profiles are shown. Peak positions are marked as purple lines.

Table S1. Cell parameters and statistical agreement factors of M-doped and undoped LDH.

Entry	Sample	Composition	***a*** **axis (Å)**	***c*** **axis (Å)**	**Volume (Å³)**	R_p, R_{wp}, R_{F2}*
1	**B**	$[Zn_{0.61}Al_{0.39}(OH)_2](Cl)_{0.39}\cdot0.6H_2O$	3.0864(8)	23.269(1)	191.9(1)	0.074, 0.100, 0.13
2	**Ir-1**	$[Zn_{0.647}Al_{0.349}Ir_{0.004}(OH)_2](Cl)_{0.353}\cdot0.6H_2O$	3.0865(7)	23.272(1)	192.0(2)	0.067, 0.087, 0.09
3	**Ru**	$[Zn_{0.65}Al_{0.33}Ru_{0.02}(OH)_2](Cl)_{0.35}\cdot0.6H_2O$	3.0955(9)	23.405(1)	194.2(1)	0.067, 0.089, 0.07
4	**Ir-2**	$[Mg_{0.647}Al_{0.349}Ir_{0.004}(OH)_2](Cl)_{0.353}\cdot0.6H_2O$	3.0511(1)	22.984(2)	185.3(2)	0.056, 0.076, 0.11

*R_p = Σ |Io-Ic| / Σ Io; R_{wp} = [Σ w(Io-Ic)2 / Σ wIo2]1/2 ; R_{F2} = Σ |Fo2 - Fc2| / Σ |Fo|

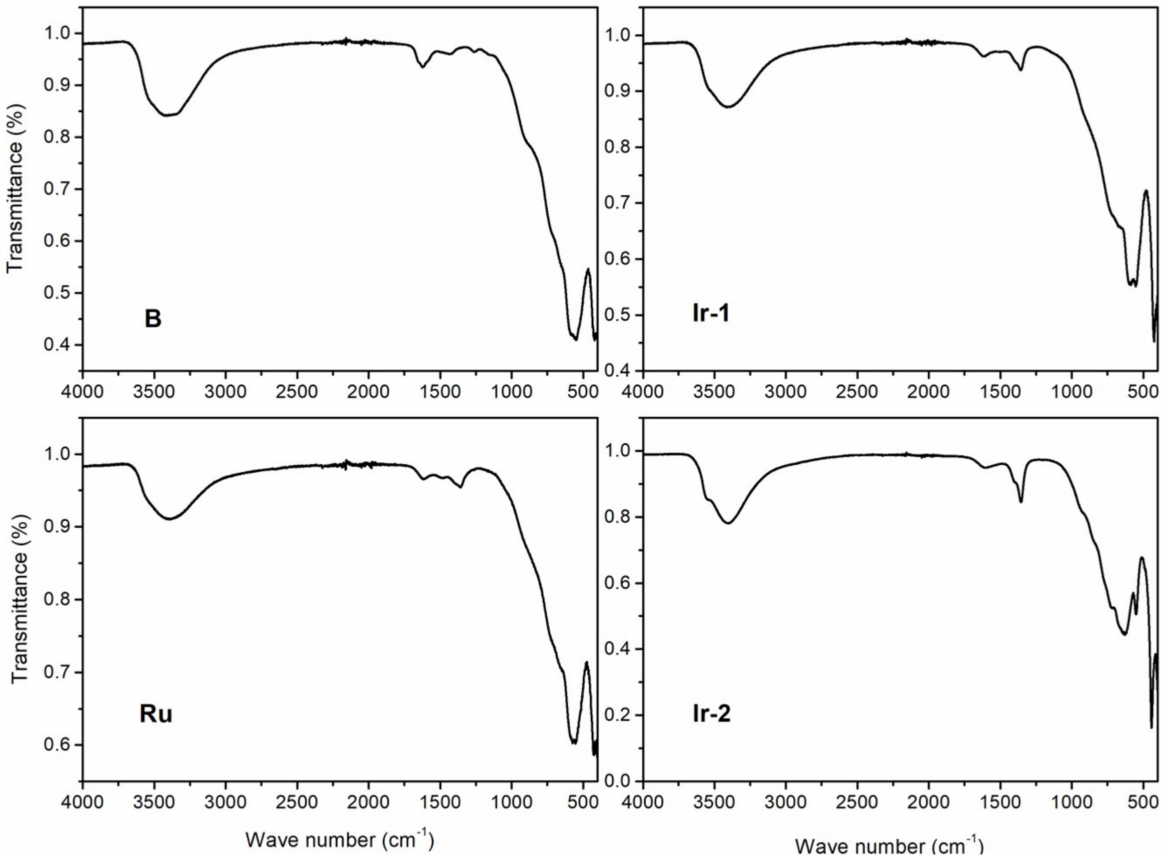

Fig. S5 FT-IR spectra of undoped LDH (**B**) and the three doped M-LDH (**Ir-1**, **Ru** and **Ir-2**). Relevant modes: water bending at 1615 cm^{-1}, O-H stretching at 3400 cm^{-1}, O-M bending at 560 cm^{-1}, carbonate at 1414 cm^{-1} (minor).

Table S2. Summary of relevant vibration modes detected by FT-IR spectroscopy (see also Fig. S5).*

Mode	**Wave number (cm^{-1})**			
	B	**Ir-1**	**Ru**	**Ir-2**
H_2O	1624	1618	1614	1605
O–H	3404	3400	3404	3408
CO_3^{2-}	1414	1357	1364	1355
O–M	567	576	567	633

*water bending, O–H stretching, O–M bending, carbonate (minor). Resolution: 1 cm^{-1}; sample scan time: 16 scans; backgroud scan time: 16 scans; aquisition from 4000 to 400 cm^{-1}.

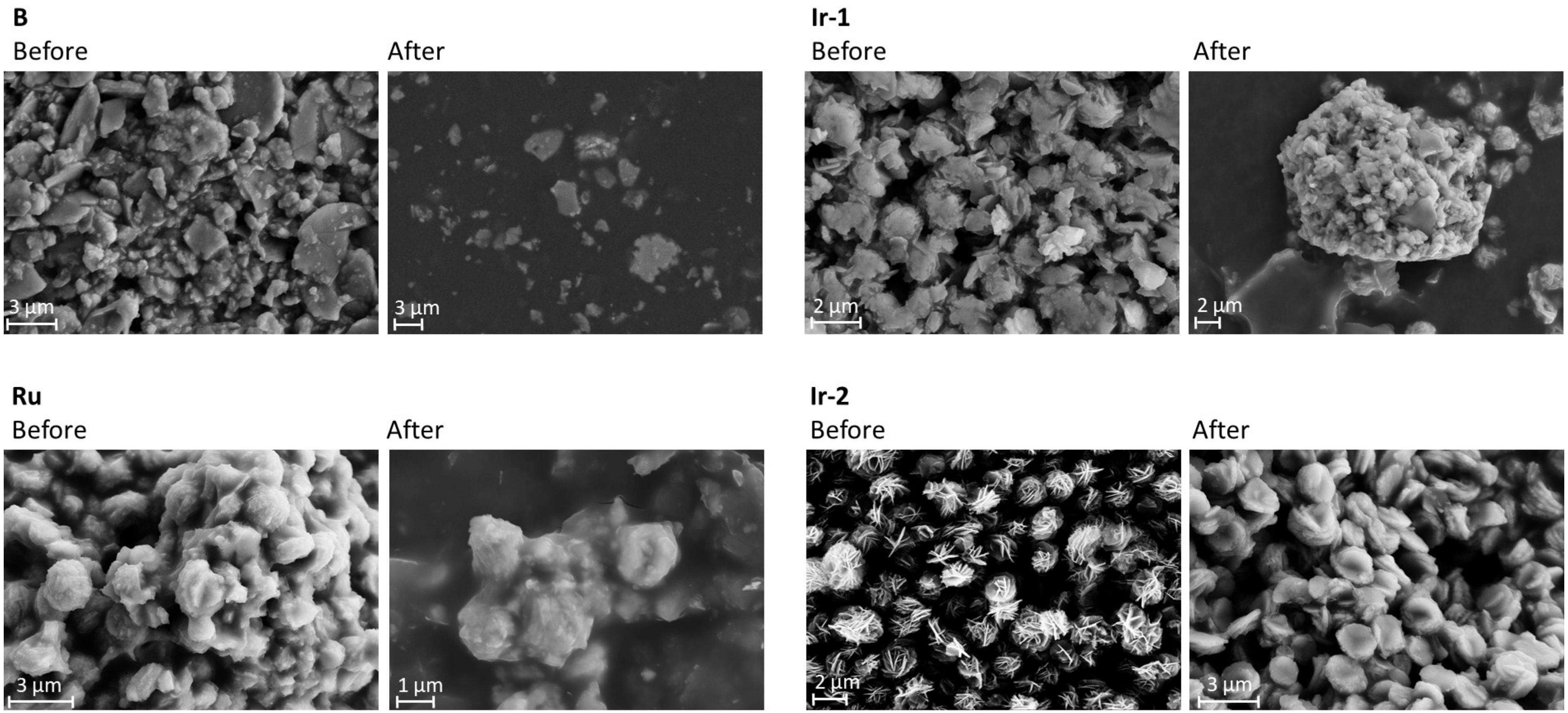

Fig. S6 SEM images of undoped LDH (**B**) and the three doped M-LDH (**Ir-1**, **Ru** and **Ir-2**) before and after catalysis. The images obtained after catalytic tests are slightly more unfocused due to the presence of residual paraffin wax of the electrode material.

- **GC analysis**

The formation of molecular oxygen was probed by GC analysis of the gas evolved in chronoamperometric experiments carried out at a constant overpotential of 700 mV over 12 h. The representative cases of **Ir-1** and **Ru** were considered. The current fluctuations in Fig. S7 are ascribed to bubbles accumulation on the electrode surface.

Details of GC analysis: Prior to GC measurements, the solution was deaerated with Ar for 30 min. During the electrochemical water oxidation experiments, the solution was kept under Ar atmosphere and stirring. A 200 µL gas sample was taken with a gas-tight micro-liter syringe (Hamilton-1825RN) and transferred to the GC injection port. After pushing the syringe bar to the 150 µL mark, 150 µL of the gas sample was quickly injected into the GC (Agilent Technologies 7820A) equipped with a thermal conductivity detector (TCD, Varian). O_2 and N_2 were separated by passing the sample through a 3 m x 2 mm packed 5 Å molecular sieve 13X 80-100 column with a helium carrier gas (purity 6.0). Only O_2 was detected for **Ir-1**. A tiny N_2 peak was detected for the **Ru** samples and belongs to air contamination, which was inevitably inserted into the needle of the syringe.

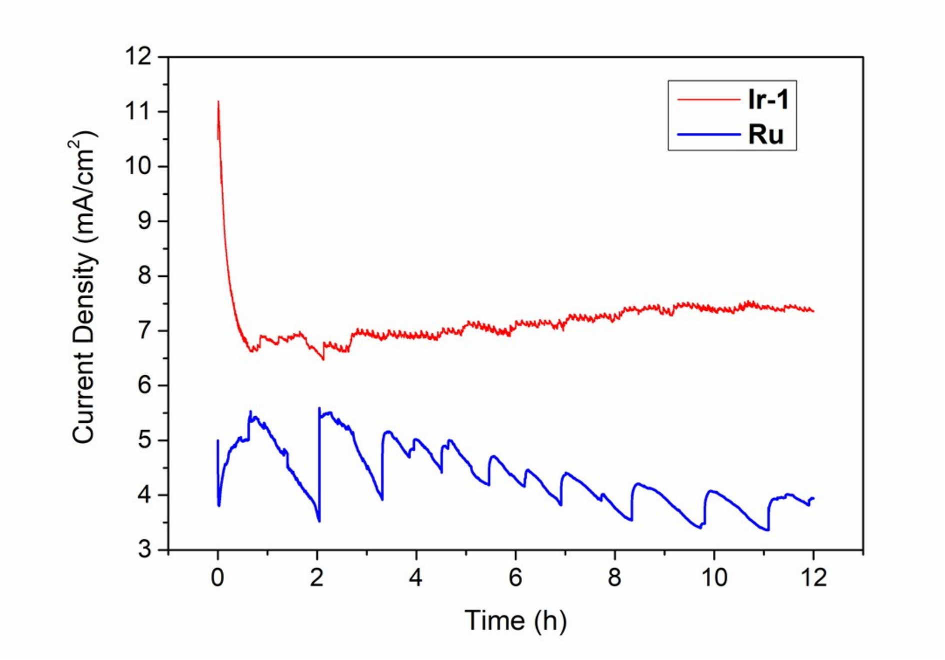

Fig. S7. Current density *vs.* time profiles obtained by chronoamperometry at an overpotential of 700 mV in 1 M KOH.

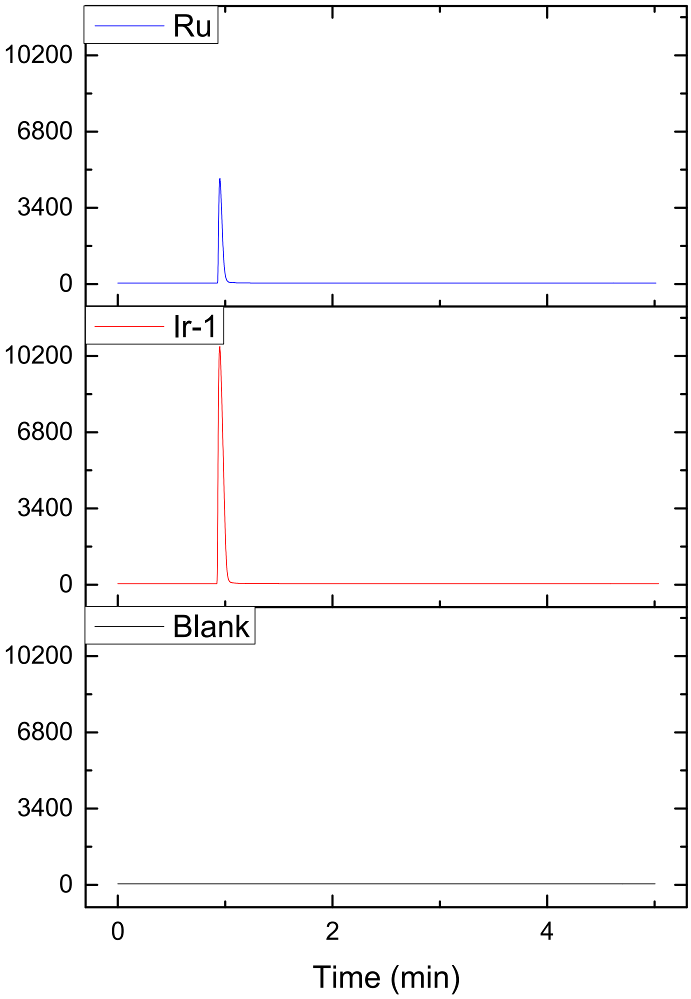

Fig. S8. GC traces relative to the chronoamperometric experiments shown in Fig. S7.

- **Tafel plots**

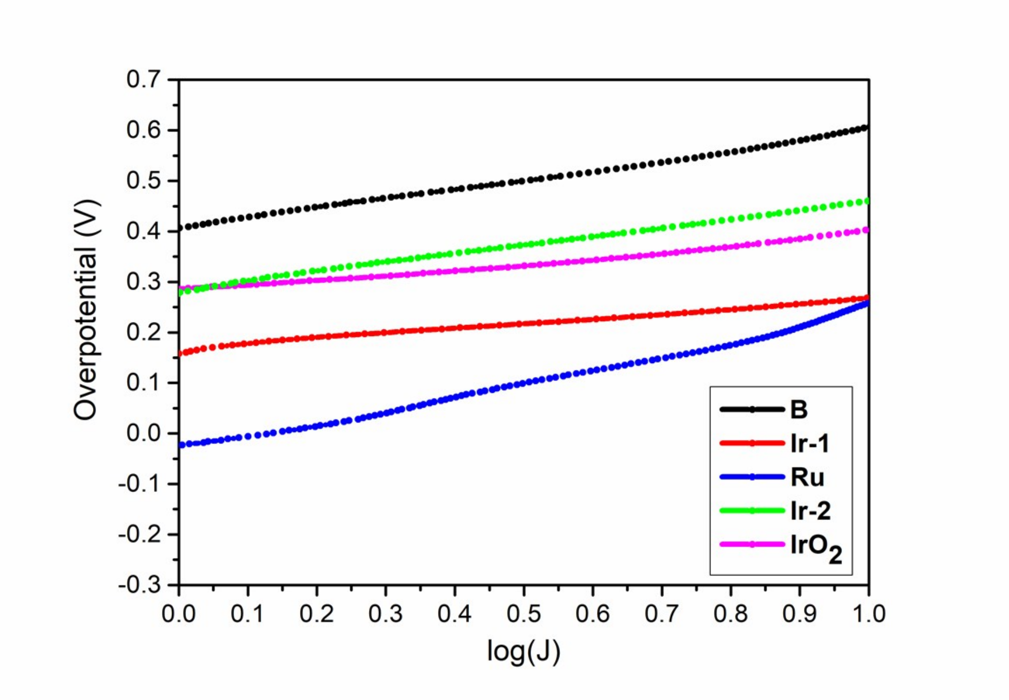

Fig. S9 Tafel plots for representative WO experiments, evaluated in the linear region 0 < log(J) < 1 for **B** and the three M-LDHs.

- **LSV curves recorded before and after chronoamperometric/chronopotentiometric measurements**

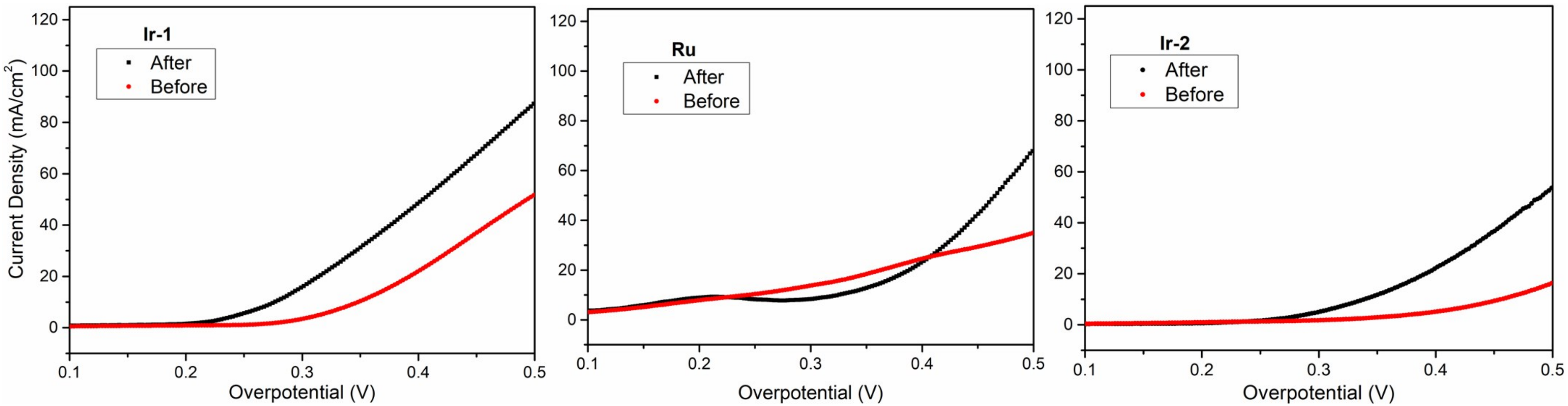

Fig. S10 Relevant regions of LSV curves recorded in WO experiments before (red) and after (black) chronoamperometric measurements (25°C, 1 M KOH, scan rate 1 mV/sec).

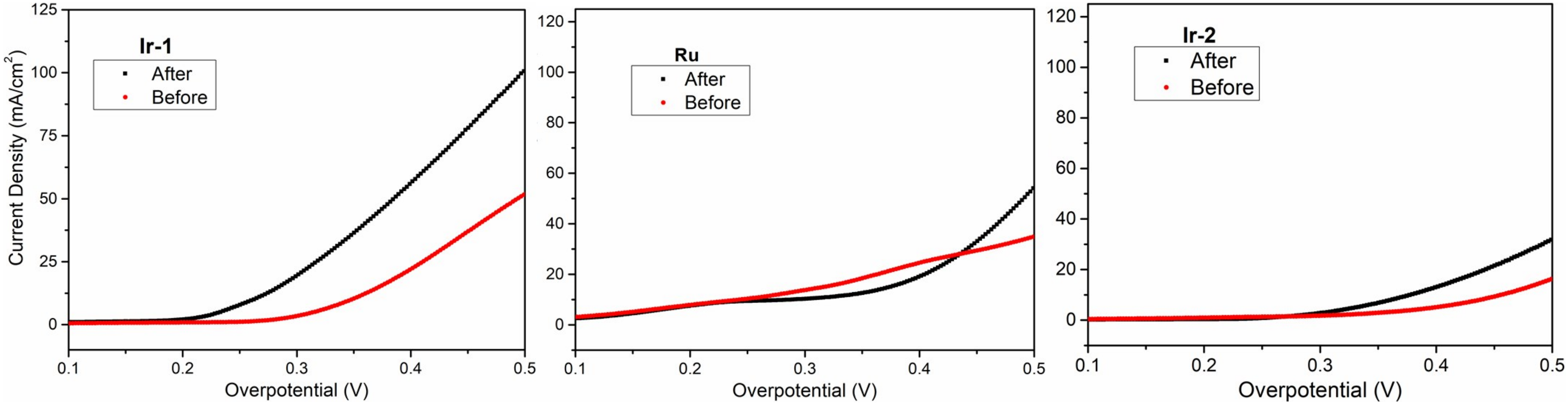

Fig. S11 Relevant regions of LSV curves recorded in WO experiments before (red) and after (black) chronopotentiometric measurements (25°C, 1 M KOH, scan rate 1 mV/sec).

- **Representative LDH-based WOCs reported in the literature**

Table S3. Summary of representative η_{10} values reported for selected LDH-based WOCs.

System	η_{10} (mV)	Ref.
NiFe LDH nanosheets by PLA	280	6,7
Ti/La-doped NiFe LDH by PLA	260	6,7
Porous NiCoFe LTH	239	8
Cr-doped NiFe LDH	280	9
Ce-doped NiFe LDH	227	10
Au-doped NiFe LDH	237	11
NiFe LDH hollow microspheres	239	12
CoMn LDH ultrathin nanoplates	~300	12
NiFe LDH @ graphene oxide	~250	13

- **References**

1 L. Fagiolari, A. Scafuri, F. Costantino, R. Vivani, M. Nocchetti and A. Macchioni, *ChemPlusChem*, 2016, **81**, 1060–1063.

2 M. Bastianini, D. Costenaro, C. Bisio, L. Marchese, U. Costantino, R. Vivani and M. Nocchetti, *Inorg. Chem.*, 2012, **51**, 2560–2568.

3 U. Costantino, F. Marmottini, M. Nocchetti and R. Vivani, *Eur. J. Inorg. Chem.*, 1998, **1998**, 1439–1446.

4 H. M. Rietveld, *J. Appl. Crystallogr.*, 1969, **2**, 65–71.

5 C. Larson, R. B. von Dreele *Generalized Crystal Structure Analysis System*. Los Alamos National Laboratory, Los Alamos, NM. 2001.

6 B. M. Hunter, J. D. Blakemore, M. Deimund, H. B. Gray, J. R. Winkler and A. M. Müller, *J. Am. Chem. Soc.*, 2014, **136**, 13118–13121.

7 B. M. Hunter, W. Hieringer, J. R. Winkler, H. B. Gray and A. M. Müller, *Energy Environ. Sci.*, 2016, **9**, 1734–1743.

8 A.-L. Wang, H. Xu and G.-R. Li, *ACS Energy Lett.*, 2016, **1**, 445–453.

9 Y. Yang, L. Dang, M. J. Shearer, H. Sheng, W. Li, J. Chen, P. Xiao, Y. Zhang, R. J. Hamers and S. Jin, *Adv. Energy Mater.*, 2018, **8**, 1703189.

10 H. Xu, B. Wang, C. Shan, P. Xi, W. Liu and Y. Tang, *ACS Appl. Mater. Inter.*, 2018, **10**, 6336–6345.

11 J. Zhang, J. Liu, L. Xi, Y. Yu, N. Chen, S. Sun, W. Wang, K. M. Lange and B. Zhang, *J. Am. Chem. Soc.*, 2018, **140**, 3876–3879.

12 C. Zhang, M. Shao, L. Zhou, Z. Li, K. Xiao and M. Wei, *ACS Appl. Mater. Interfaces*, 2016, **8**, 33697–33703.

13 F. Song and X. Hu, *J. Am. Chem. Soc.*, 2014, **136**, 16481–16484.